

Supporting Information
For

Intramolecular Charge Transfer and Ion Pairing in *N,N*-Diaryl Dihydrophenazine Photoredox Catalysts for Efficient Organocatalyzed Atom Transfer Radical Polymerization

Chern-Hooi Lim,^{†*a*} Matthew D. Ryan,^{†*a*} Blaine G. McCarthy,^{*a*} Jordan C. Theriot,^{*a*} Steven M. Sartor,^{*a*} Niels H. Damrauer,^{*a,c*} Charles B. Musgrave,^{*a,b,c*} Garret M. Miyake^{*a,c*}

^{*a*}Department of Chemistry and Biochemistry, ^{*b*}Department of Chemical and Biological Engineering. ^{*c*}Materials Science and Engineering Program, University of Colorado Boulder, Boulder, Colorado 80309, USA.

*Corresponding author, E-mail: garret.miyake@colorado.edu

Table of Contents

1. Materials & Methods	3
2. Procedures	4
a) General Polymerization Procedure	4
b) Solvent System Optimization.....	4
3. Computational Details	5
a) Excited State Calculation.....	5
b) Orbital Energy.....	9
c) Electrostatic Potential (ESP) Calculation.....	9
d) Complexation Free Energy of ${}^2\text{PC}^{\bullet+}$ and Br^-	9
4. Solvatochromic Determination of Dipole Moment	11
5. Supplementary Polymerization Data: <i>M2BP Initiator</i>	13
6. Supplementary Polymerization Data: <i>DBMM Initiator</i>	14
7. UV-vis Spectrum of PC 2 in Solvents of Varying Polarity	16
8. Oxidation of P_n^{\bullet} by ${}^2\text{PC}^{\bullet+}\text{Br}^-$ Ion Pair	17
9. Oxygen Quenching on PC 3's Emission Spectrum	18
10. Coordinates of Molecular Structures	19
a) Br^-	19
b) ${}^2\text{PC}^{\bullet+}\text{Br}^-$ (PC 3).....	19
c) ${}^2\text{PC}^{\bullet+}$ (PC 3).....	21
d) $\text{NBu}_4^+\text{Br}^-$	23
e) NBu_4^+	25
11. References.....	28

1. Materials & Methods

General Information

All reagents were purchased from Sigma-Aldrich. Monomers and solvents used in polymerizations: methyl methacrylate (MMA), dimethylacetamide (DMA), were dried over CaH₂, purified by vacuum distillation, and degassed by 20 minutes of N₂ sparging before storage and subsequent use in a N₂ glovebox. Spectral grade tetrahydrofuran (THF) and dimethylformamide (DMF) were purified using a Mbraun solvent system and used without further treatment. 1-hexene, benzene, and dioxane were used as received. Monomers were stored at -34 °C in the glovebox freezer and allowed to warm to room temperature before use in polymerizations.

Alkyl halide initiators used in polymerizations: methyl 2-bromopropionate (M2BP) and diethyl 2-bromo-2-methylmalonate (DBMM) were purified by vacuum distillation and degassed by three freeze-pump-thaw cycles before storage and subsequent use in a N₂ glovebox. Initiators were stored at -34 °C in the glovebox freezer and allowed to warm to room temperature before use in polymerizations.

Reagents used in the synthesis of organic photocatalysts: 2-Dicyclohexylphosphino-2,6-diisopropoxybiphenyl (RuPhos) and Chloro-(2-Dicyclohexylphosphino-2,6-diisopropoxy-1,1-biphenyl) [2-(2-aminoethyl)phenyl] palladium(II) – methyl-t-butyl ether adduct (RuPhos precatalyst, 1st generation) were stored and used in N₂ glovebox. All other reagents were used as received without further treatment.

The visible light irradiation source was white LEDs (16-inch strip, double-density white LEDs), purchased from Creative Lighting Solutions (item no. CL-FRS1210-5M-12V-WH), wrapped inside of an aluminum foil lined 400mL beaker.

¹H, ¹³C, and ¹⁹F NMR spectroscopy were obtained from either a Varian INOVA 400 MHz, 500 MHz, or Bruker 300MHz spectrometer. Chemical shifts referenced to an internal solvent resonance as parts-per-million (ppm) relative to tetramethylsilane. Deuterated solvents were purchased from Cambridge Isotope Labs and used as received. Polymer molecular weights were obtained *via* gel permeation chromatography (GPC) coupled with multi-angle light scattering (MALS), using an Agilent HPLC fitted with one guard column and three PLgel 5 μm MIXED-C gel permeation columns, a Wyatt Technology TrEX differential refractometer, and a Wyatt Technology miniDAWN TREOS light scattering detector, using THF as the eluent at a flow rate of 1.0mL/min. Ultraviolet-visible spectroscopy (UV-Vis) was performed on an Agilent Cary 5000 spectrophotometer. Emission spectroscopy was performed on a SLM 8000C spectrofluorimeter; samples sparged with argon for 15 minutes prior to data acquisition. Electrospray Ionization Mass Spectrometry (ESI-MS) and was performed at the University of Colorado-Boulder Central Analytical Mass Spectrometry Facility on a Waters Synapt G2 HDMS Qtof with MeCN as the solvent.

2. Procedures

a) General Polymerization Procedure

A 20 mL scintillation vial with a plastic-lined cap was charged with a small stirbar and photocatalyst (4.00 mg, 9.35 μmol , 1 eq), and transferred to a N₂ glovebox. DMA (1.50 mL), THF (0.50 mL), MMA (1.00 mL, 9.35 mmol, 1000 eq), and DBMM (17.9 μL , 93.5 μmol , 10 eq) were added sequentially *via* pipette. The vial was then quickly sealed and placed into the beaker with white LEDs and stirred for 8 hours. To track the progression of the polymerization, 0.1mL aliquots were removed *via* syringe at 1-hour increments, and injected into a sealed HPLC vial containing 0.7 mL of CDCl₃ with 250 ppm butylated hydroxytoluene (BHT) additive. This aliquot was analyzed by ¹H NMR to analyze the monomer conversion and then dried to remove the volatiles. The dried sample was re-dissolved in spectral grade THF for analysis by GPC coupled with MALS.

b) Solvent System Optimization

The selected solvent systems were: 100/0, 75/25, 50/50, 25/75, 0/100 by volume (DMA/THF). The progression of all polymerizations was tracked in the same way as for those in the *General Polymerization Procedure*. An overall 2:1 solvent:monomer volume ratio (v:v) was maintained for the different solvent systems. The data for these experiments are presented in the *Supplementary Polymerization Data* section.

3. Computational Details

All calculations were performed using computational chemistry software package Gaussian 09 ver. D01.¹ We acknowledge the use of computational resource provided by XSEDE - Comet supercomputer.

a) Excited State Calculation

Ground state geometries of PC **1**, **2** and **3** were obtained from previous calculations² computed at uM06/6-31+G(d,p)/CPCM-H₂O level of theory.³ Using these geometries, single point time dependent density functional theory (TD-DFT) calculations were performed using the rCAM-B3LYP/6-31+G(d,p)/CPCM-DMA level of theory.⁴ rCAM-B3LYP was chosen because it gave better λ_{max} predictions that are closer to experimental values in comparison to rwB97xd level of theory; however, both of these methods gave similar results in terms of contributions of local excitation (LE) and charge transfer (CT) in the initial photoexcitation. The first 10 excited states of PC **1**, **2**, and **3** are reported below. Dominant UV-vis absorption peaks with significant and relevant oscillator strengths (f value) are highlighted.

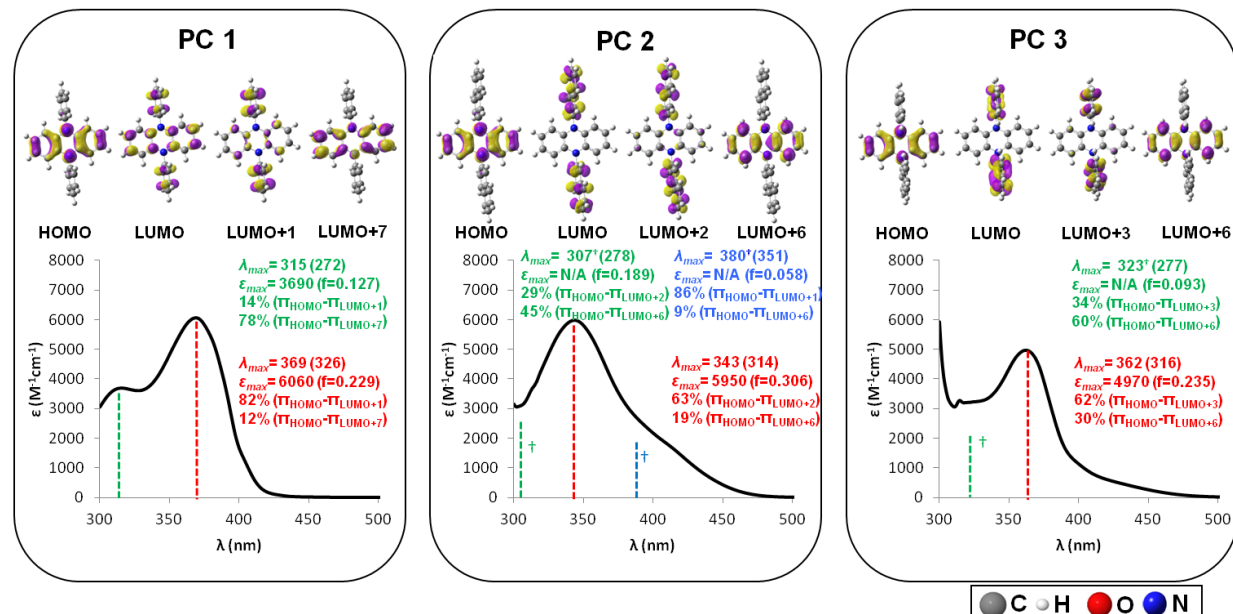


Figure S1. UV-vis spectra of PC **1**, **2**, and **3** (in DMA) along with theoretically assigned orbital contributions to observed electronic transitions. † Predicted wavelength of hidden peaks.

PC 1

Excited State 1: Singlet-A 3.4017 eV 364.47 nm $f=0.0000$ $\langle S^{**2} \rangle=0.000$

88 -> 89	0.62220
88 -> 94	-0.31360

Excited State 2: Singlet-A 3.8009 eV 326.20 nm $f=0.2292$ $\langle S^{**2} \rangle=0.000$

87 -> 89	0.13082
88 -> 90	0.63929 ($\pi_{\text{HOMO}} \cdot \pi_{\text{LUMO}+1}$, $2*(0.63929)^2 * 100 = 82\%$ contribution)
88 -> 96	0.24989 ($\pi_{\text{HOMO}} \cdot \pi_{\text{LUMO}+7}$, 12% contribution)

Excited State 3: Singlet-A 3.9447 eV 314.31 nm f=0.0000 <S**2>=0.000
87 -> 92 -0.12845
88 -> 91 0.68214

Excited State 4: Singlet-A 3.9843 eV 311.18 nm f=0.0048 <S**2>=0.000
87 -> 91 -0.13516
88 -> 92 0.67915

Excited State 5: Singlet-A 4.2367 eV 292.65 nm f=0.0008 <S**2>=0.000
88 -> 93 0.46039
88 -> 97 -0.45803
88 ->100 0.13505
88 ->101 0.15853

Excited State 6: Singlet-A 4.3213 eV 286.92 nm f=0.0020 <S**2>=0.000
88 -> 93 0.41284
88 -> 97 0.46387
88 -> 99 0.13330
88 ->101 0.24115

Excited State 7: Singlet-A 4.3981 eV 281.91 nm f=0.0000 <S**2>=0.000
87 -> 90 0.13676
88 -> 89 0.31306
88 -> 94 0.61150

Excited State 8: Singlet-A 4.5616 eV 271.80 nm f=0.1268 <S**2>=0.000
87 -> 94 -0.13898
88 -> 90 -0.26664 ($\pi_{\text{HOMO}}-\pi_{\text{LUMO+1}}$, 14% contribution)
88 -> 96 0.62461 ($\pi_{\text{HOMO}}-\pi_{\text{LUMO+7}}$, 78% contribution)

Excited State 9: Singlet-A 5.0577 eV 245.14 nm f=0.0000 <S**2>=0.000
88 -> 97 0.16644
88 -> 99 -0.43523
88 ->100 0.45641
88 ->107 0.22361

Excited State 10: Singlet-A 5.0803 eV 244.05 nm f=0.0001 <S**2>=0.000
88 -> 98 0.67080
88 ->113 -0.13676

PC 2

Excited State 1: Singlet-A 3.4371 eV 360.73 nm f=0.0000 <S**2>=0.000
114 ->115 0.52456
114 ->118 0.16236
114 ->119 -0.42658

Excited State 2: Singlet-A 3.5334 eV 350.90 nm f=0.0576 <S**2>=0.000
111 ->115 0.11053
114 ->116 0.65605 ($\pi_{\text{HOMO}}-\pi_{\text{LUMO+1}}$, 86% contribution)
114 ->121 -0.20734 ($\pi_{\text{HOMO}}-\pi_{\text{LUMO+6}}$, 9% contribution)

Excited State 3: Singlet-A 3.6890 eV 336.09 nm f=0.0000 <S**2>=0.000
114 ->115 0.40605
114 ->118 -0.38413
114 ->119 0.36653

114 ->125 0.15114

Excited State 4: Singlet-A 3.9476 eV 314.08 nm f=0.3058 <S**2>=0.000
114 ->117 0.56126 ($\pi_{\text{HOMO}}-\pi_{\text{LUMO+2}}$, 63% contribution)
114 ->121 0.30706 ($\pi_{\text{HOMO}}-\pi_{\text{LUMO+6}}$, 19% contribution)
114 ->124 0.19584
114 ->130 0.11703

Excited State 5: Singlet-A 4.2124 eV 294.33 nm f=0.0033 <S**2>=0.000
114 ->120 0.44774
114 ->123 -0.42924
114 ->127 0.26363

Excited State 6: Singlet-A 4.3266 eV 286.56 nm f=0.0000 <S**2>=0.000
111 ->117 -0.11704
114 ->115 0.15221
114 ->118 0.54188
114 ->119 0.37951

Excited State 7: Singlet-A 4.4626 eV 277.83 nm f=0.1894 <S**2>=0.000
114 ->116 0.16671
114 ->117 -0.38403 ($\pi_{\text{HOMO}}-\pi_{\text{LUMO+2}}$, 29% contribution)
114 ->121 0.47616 ($\pi_{\text{HOMO}}-\pi_{\text{LUMO+6}}$, 45% contribution)
114 ->124 0.21307
114 ->130 0.12695

Excited State 8: Singlet-A 4.4718 eV 277.26 nm f=0.0348 <S**2>=0.000
114 ->120 0.42463
114 ->123 0.30228
114 ->126 -0.24083
114 ->127 -0.29061
114 ->129 -0.15481
114 ->134 0.10264

Excited State 9: Singlet-A 4.5617 eV 271.79 nm f=0.0732 <S**2>=0.000
112 ->115 0.47529
113 ->116 0.47719

Excited State 10: Singlet-A 4.5646 eV 271.62 nm f=0.2685 <S**2>=0.000
112 ->116 0.46511
113 ->115 0.47435

PC 3

Excited State 1: Singlet-A 3.2951 eV 376.26 nm f=0.0006 <S**2>=0.000
111 ->116 -0.11194
114 ->115 0.68293

Excited State 2: Singlet-A 3.2994 eV 375.78 nm f=0.0001 <S**2>=0.000
111 ->115 -0.11294
114 ->116 0.68297

Excited State 3: Singlet-A 3.4583 eV 358.51 nm f=0.0000 <S**2>=0.000
114 ->117 0.54297
114 ->119 0.43295

Excited State 4: Singlet-A 3.9264 eV 315.77 nm f=0.2348 <S**2>=0.000

111 ->117 0.12212
 114 ->118 0.55789 ($\pi_{\text{HOMO}}-\pi_{\text{LUMO}+3}$, 62% contribution)
 114 ->121 0.38533 ($\pi_{\text{HOMO}}-\pi_{\text{LUMO}+6}$, 30% contribution)

Excited State 5: Singlet-A 4.2086 eV 294.60 nm f=0.0039 <S**2>=0.000
 114 ->120 0.32888
 114 ->122 0.51724
 114 ->124 -0.23782

Excited State 6: Singlet-A 4.3984 eV 281.89 nm f=0.0000 <S**2>=0.000
 111 ->118 -0.11515
 114 ->117 -0.43405
 114 ->119 0.53821

Excited State 7: Singlet-A 4.4798 eV 276.76 nm f=0.0928 <S**2>=0.000
 111 ->119 0.12675
 114 ->118 -0.40986 ($\pi_{\text{HOMO}}-\pi_{\text{LUMO}+3}$, 34% contribution)
 114 ->121 0.54780 ($\pi_{\text{HOMO}}-\pi_{\text{LUMO}+6}$, 60% contribution)

Excited State 8: Singlet-A 4.5164 eV 274.52 nm f=0.0007 <S**2>=0.000
 112 ->115 0.16157
 113 ->116 -0.16123
 114 ->120 0.49491
 114 ->122 -0.14153
 114 ->124 0.15330
 114 ->126 -0.25117
 114 ->127 -0.12869
 114 ->128 0.15964
 114 ->136 0.14175

Excited State 9: Singlet-A 4.5372 eV 273.26 nm f=0.4513 <S**2>=0.000
 112 ->116 -0.47673
 113 ->115 0.48817

Excited State 10: Singlet-A 4.5843 eV 270.45 nm f=0.0035 <S**2>=0.000
 112 ->115 -0.43341
 113 ->116 0.43520
 114 ->120 0.13311
 114 ->122 -0.13453

For PC **1**, the "red" peak was experimentally determined to have maximum absorption wavelength (λ_{max}) of 369 nm and molar absorptivity at λ_{max} (ϵ_{max}) of $6060 \text{ M}^{-1}\text{cm}^{-1}$ (Figure S1). TD-DFT predictions generally underestimated λ_{max} values of dihydrophenazine derivatives, where the "red" peak of PC **1** was predicted to be $\lambda_{\text{max,calc}} = 326 \text{ nm}$ with its oscillator strength (f) of 0.229. This peak was theoretically assigned to be contributed by 82% $\pi_{\text{HOMO}}-\pi_{\text{LUMO}+1}$ and 12% $\pi_{\text{HOMO}}-\pi_{\text{LUMO}+7}$ transitions. A second "green" peak of PC **1** at $\lambda_{\text{max}} = 315 \text{ nm}$ ($\epsilon_{\text{max}} = 3690 \text{ M}^{-1}\text{cm}^{-1}$) was also identified, which was predicted to have $\lambda_{\text{max,calc}} = 272 \text{ nm}$ (f = 0.127) and contributed by 14% $\pi_{\text{HOMO}}-\pi_{\text{LUMO}+1}$ and 78% $\pi_{\text{HOMO}}-\pi_{\text{LUMO}+7}$ transitions.

For PC **2**, the main "red" peak was measured at $\lambda_{\text{max}} = 343 \text{ nm}$ ($\epsilon_{\text{max}} = 5950 \text{ M}^{-1}\text{cm}^{-1}$) and was predicted to be $\lambda_{\text{max,calc}} = 314 \text{ nm}$ (f = 0.306). We theoretically identified two hidden peaks, "green" and "blue" peaks, with $\lambda_{\text{max, calc}} = 278 \text{ nm}$ and $\lambda_{\text{max, calc}} = 351 \text{ nm}$, respectively. These

hidden peaks (with smaller molar absorptivity) were over signaled by the other peaks that they were not observed as distinctive peaks in the UV-vis spectrum. Using the relative shift between λ_{max} and $\lambda_{\text{max, calc}}$ of the "red" peak ($\Delta\lambda = 29$ nm), the hidden "green" and "blue" peaks were predicted to reside at 307 nm and 380 nm, respectively. π_{HOMO} , $\pi_{\text{LUMO+1}}$, $\pi_{\text{LUMO+2}}$, and $\pi_{\text{LUMO+6}}$ orbitals with varying contributions were involved in PC **2**'s electronic transitions.

For PC **3**, the main "red" peak was measured at $\lambda_{\text{max}} = 362\text{nm}$ ($\epsilon_{\text{max}} = 4970 \text{ M}^{-1}\text{cm}^{-1}$) and was predicted to be $\lambda_{\text{max,calc}} = 316$ nm ($f = 0.235$). This peak was contributed by 62% $\pi_{\text{HOMO}}-\pi_{\text{LUMO+3}}$ and 30% $\pi_{\text{HOMO}}-\pi_{\text{LUMO+6}}$ transitions. A hidden "green" peak was predicted to reside at 323 nm and was predicted to be contributed by 34% $\pi_{\text{HOMO}}-\pi_{\text{LUMO+3}}$ and 60% $\pi_{\text{HOMO}}-\pi_{\text{LUMO+6}}$ transitions.

b) Orbital Energy

Converged ^1PC and $^3\text{PC}^*$ geometries of PC **1**, **2** and **3** were obtained from previous calculations² computed at uM06/6-31+G(d,p)/CPCM-H₂O level of theory. Using these geometries, single point energy calculations were performed at uM06/6-311+G(d,p)/CPCM-DMA level of theory to obtain the orbital energies of PC **1**, **2**, and **3** (π_{HOMO} , π_{SOMO} , π_{LUMO} , and $\pi_{\text{LUMO+n}}$, where n = 1 -7).

c) Electrostatic Potential (ESP) Calculation

Converged ^1PC and $^3\text{PC}^*$ geometries of PC **1**, **2** and **3** were obtained from previous calculations² computed at uM06/6-31+G(d,p)/CPCM-H₂O level of theory. Using these geometries, single point energy calculations with CHELPG⁵ ESP population analysis were performed at uM06/6-31G(d,p)/CPCM-DMA level of theory. Total electron density of ^1PC and $^3\text{PC}^*$ were first plotted and then were mapped with ESP derived charges to show distribution of charges on the dihydrophenazine derivatives.

d) Complexation Free Energy of $^2\text{PC}^{\bullet+}$ and Br⁻

Geometries of $^2\text{PC}^{\bullet+}$, Br⁻, and ion pair $^2\text{PC}^{\bullet+}\text{Br}^-$ were optimized at uM06/6-31+G(d,p)/CPCM-DMA level of theory followed by frequency calculations to obtain zero point energy (ZPE) corrections, thermal corrections, and entropic TS terms using ideal gas approximations. The obtained Gibbs free energy, $G^0(298 \text{ K}, 1 \text{ atm})$, by default has a standard reference state of 298.15K and 1 atm. However, a standard reference state of 298.15K and 1 mole/liter [$G^0(298 \text{ K}, 1\text{M})$] is more relevant to our examined systems as the O-ATRP reactions are carried out in the liquid phase in DMA or THF.

To obtain the Gibbs free energy with relevant standard state reference, $G^0(298 \text{ K}, 1 \text{ M}) = G^0(298 \text{ K}, 1 \text{ atm}) + RT \ln(0.08206 \text{ T})$, where R is the gas constant and T is the temperature. $\Delta G^0(298 \text{ K}, 1 \text{ M}) = \Delta G^0(298 \text{ K}, 1 \text{ atm})$ when there is no mole change to the product from the reactant. However, the reaction of $^2\text{PC}^{\bullet+} + \text{Br}^- = ^2\text{PC}^{\bullet+}\text{Br}^-$ has one net mole change and $\Delta G^0(298 \text{ K}, 1 \text{ M}) = \Delta G^0(298 \text{ K}, 1 \text{ atm}) - 1.89 \text{ kcal/mol}$.

At the converged geometries, single point calculations at uM06/6-311+G(d,p)/CPCM-DMA were performed; the various corrections and entropic TS terms from uM06/6-31+G(d,p) calculations will then be applied to the energy obtained with uM06/6-311+G(d,p). Similar procedures were performed using THF, described by CPCM solvent model.

The just-described computational methods were benchmarked against available experimental values for the complexation free energy between tetrabutylammonium cation (NBu₄⁺) and Br⁻ in

DMA and THF.⁶ Our methods correctly predicted the trend of stronger complexation between NBu₄⁺ and Br⁻ in THF versus DMA; in addition, our methods satisfactorily reproduced the experimental $\Delta G^0_{\text{complex}}$ values to within < 1.5 kcal/mol (Figure S2).

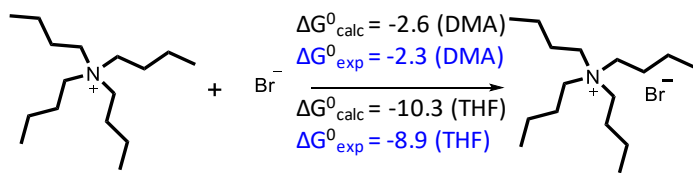


Figure S2. Experimental and predicted complexation free energy between NBu₄⁺ and Br⁻ in THF and DMA.

4. Solvatochromic Determination of Dipole Moment

The sensitivity of the maximum wavelength of emission to changes in solvent polarity can be related to the change in dipole moment between the ground and excited state using the Lippert equation:⁷

$$\Delta\nu = \frac{2}{hc} \frac{\Delta\mu^2}{a^3} \Delta f + c$$

Where $\Delta\nu$ is the observed Stokes shift in a given solvent, h is Planck's constant, c is the speed of light, $\Delta\mu$ is the change in dipole upon excitation, a is the radius of the solvent sphere surrounding the molecule, Δf is the solvent orientation polarizability, a value derived from both the solvent's dielectric constant and refractive index, and c is a constant. A plot of $\Delta\nu$ versus Δf , referred to as a Lippert-Mataga plot, gives a slope from which $\Delta\mu$ can be extracted (Figure S3 and S4).

To estimate a , a spherical approximation, where a equals half the length of the molecule, was used for **3**. An ellipsoidal approximation, where a equals 0.4 times the length of the molecule, was used for the more elongated **2**. This gave a value for $\Delta\mu$ of 16.0 D for **3** and 22.1 D for **2**, which is in good agreement with the computationally-derived values of 17.2 D and 20.8 D, respectively.

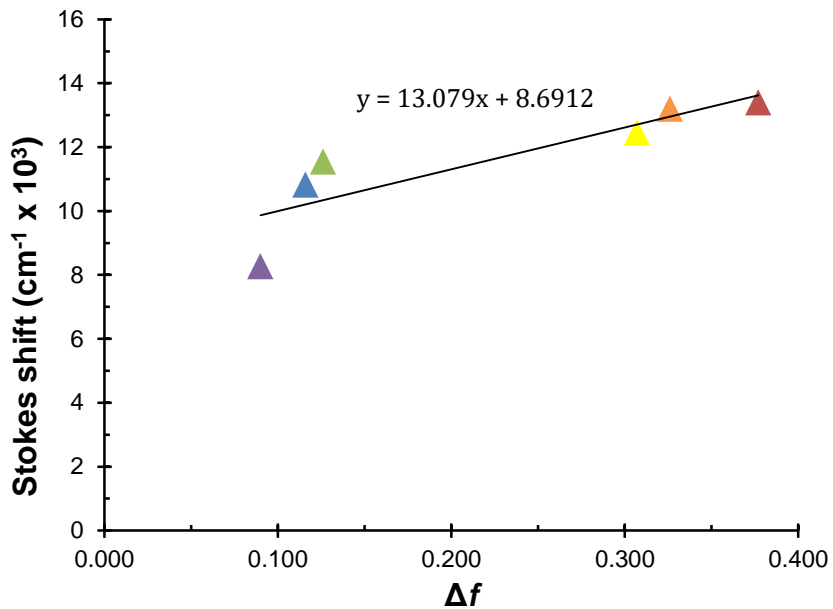


Figure S3. The Lippert-Mataga plot for PC 2, where the stokes shift ($\Delta\nu$) is plotted as a function of solvent orientation polarizability (Δf) for 1-hexene (purple), benzene (blue), dioxane (green), THF (yellow), pyridine (orange), and DMF (red).

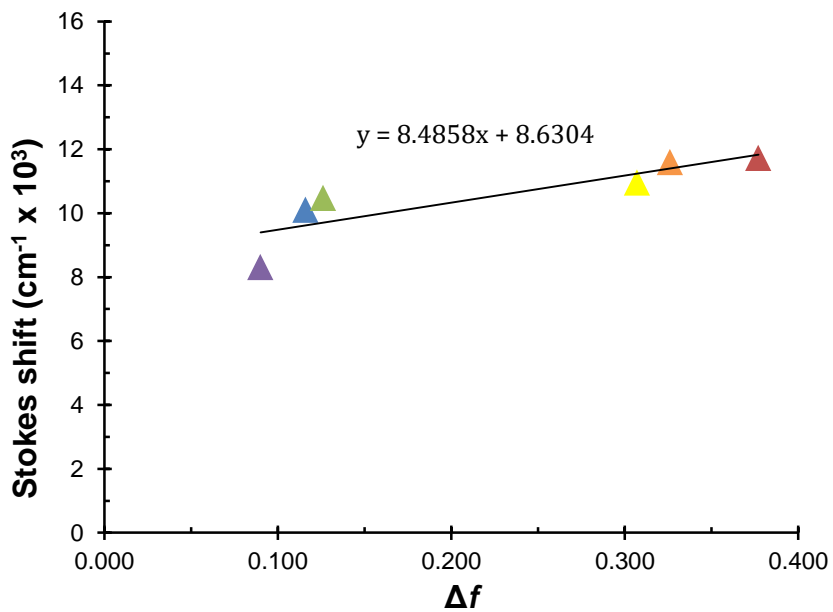


Figure S4. The Lippert-Mataga plot for PC 3, where the stokes shift ($\Delta\nu$) is plotted as a function of solvent orientation polarizability (Δf) for 1-hexene (purple), benzene (blue), dioxane (green), THF (yellow), pyridine (orange), and DMF (red).

5. Supplementary Polymerization Data: M2BP Initiator

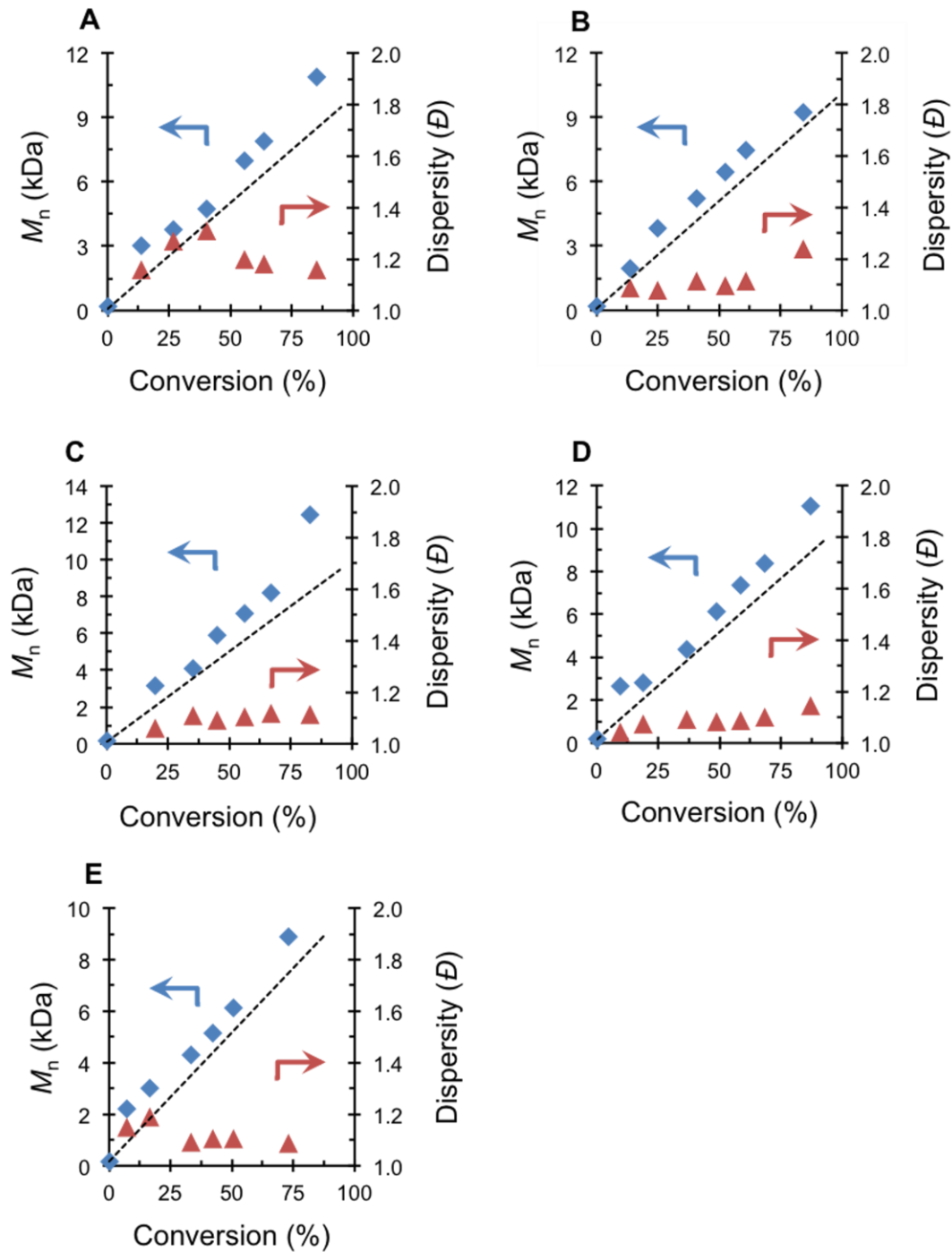


Figure S5. Plots of molecular weight (M_n , blue) and dispersity (D , red) as a function of monomer conversion for the polymerization of MMA (1000 eq, 1.00 mL, 9.35 mmol) catalyzed by PC **3** (1 eq, 4.00 mg, 9.35 μ mol), using M2BP (10 eq, 10.00 μ L, 93.5 μ mol) initiator, and 100/0 (**A**), 75/25 (**B**), 50/50 (**C**), 25/75 (**D**), 0/100 (**E**) DMA/THF solvent systems (2/1, solvent/monomer volume ratio).

6. Supplementary Polymerization Data: DBMM Initiator

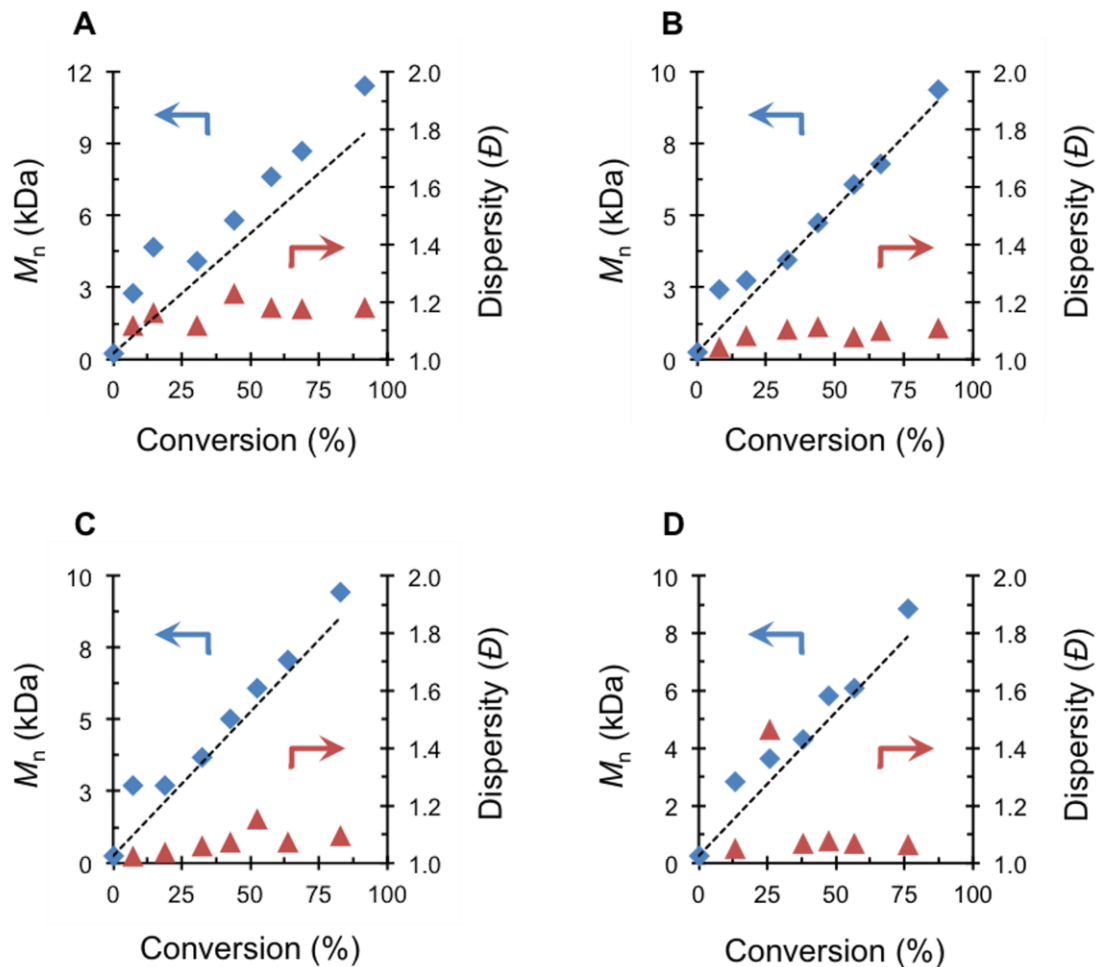


Figure S6. Plots of molecular weight (M_n , blue) and dispersity (D , red) as a function of monomer conversion for the polymerization of MMA (1000 eq, 1.00 mL, 9.35 mmol) catalyzed by PC **3** (1 eq, 4.00 mg, 9.35 μ mol), using DBMM initiator (10 eq, 18.0 μ L, 93.5 μ mol), and 100/0 (**A**), 75/25 (**B**), 50/50 (**C**), 25/75 (**D**), 0/100 (**E**) DMA/THF solvent systems (2/1, solvent/monomer volume ratio).

Table S1. Results of the O-ATRP of MMA Using PC **3** in Different Solvent Systems^a

Run No.	Initiator	Solvent Ratio (DMA/THF) ^a	Time (h)	Conversion (%) ^b	M_w (kDa) ^c	M_n (kDa) ^c	D (M_w/M_n) ^c	I^* (%) ^d
1	M2BP	100/0	8	85.14	12.6	10.9	1.16	79.7
2	M2BP	75/25	8	84.19	11.4	9.2	1.24	93.4
3	M2BP	50/50	8	82.99	13.8	12.4	1.11	68.2
4	M2BP	25/75	8	87.02	12.6	11.0	1.14	80.6
5	M2BP	0/100	8	72.90	9.7	8.9	1.09	83.9
6	DBMM	100/0	8	91.51	13.4	11.4	1.18	81.9
7	DBMM	50/50	8	87.62	10.4	9.4	1.11	95.1
8	DBMM	25/75	8	82.95	10.3	9.4	1.10	90.9
9	DBMM	0/100	8	76.10	9.5	8.9	1.07	87.8

^aSee Supporting Information section 2a and 2b for details. ^bMeasured by ¹H NMR. ^cMeasured by GPC coupled with light scattering. ^d I^* = theoretical number average MW/ experimentally measured number average MW *100.

7. UV-vis Spectrum of PC 2 in Solvents of Varying Polarity

To confirm that the solvatochromic response of PC 2 is not due to photoexcitation events, the UV-vis spectrum of PC 2 was acquired in solvents of different polarities. Regardless of the solvent, PC 2's absorption profile and λ_{max} are nearly identical (Figure S7).

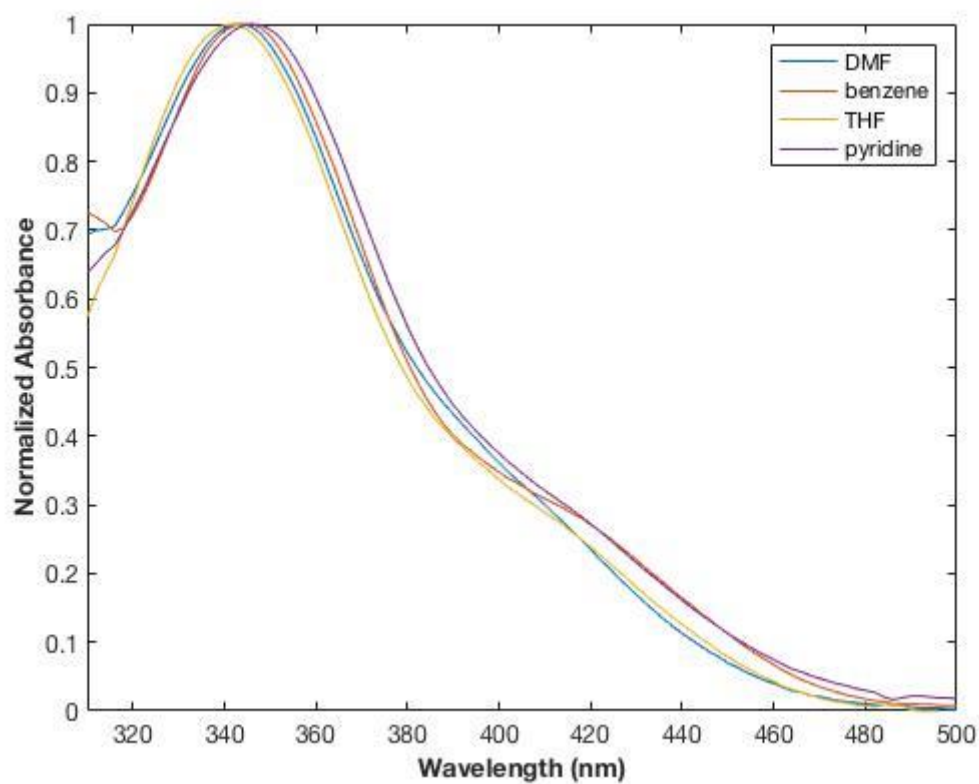


Figure S7. UV-vis spectrum of PC 2 in benzene ($\epsilon = 2.27$), THF ($\epsilon = 7.43$), pyridine ($\epsilon = 13.0$), and DMF ($\epsilon = 37.2$), where ϵ is the dielectric constant of the solvent.

8. Oxidation of $P_n\bullet$ by ${}^2PC\bullet^+Br^-$ Ion Pair

Deactivation of O-ATRP requires oxidation of $P_n\bullet$ by ${}^2PC\bullet^+$ and Br^- to reinstall the bromine chain-end group to regenerate 1PC and P_n-Br (Figure S8). We propose that ion pairing of ${}^2PC\bullet^+$ and Br^- to form ${}^2PC\bullet^+Br^-$ is essential for effective deactivation because it reduces a three-body collision to a more likely pseudo two-body collision event involving only two entities of ${}^2PC\bullet^+Br^-$ and $P_n\bullet$.

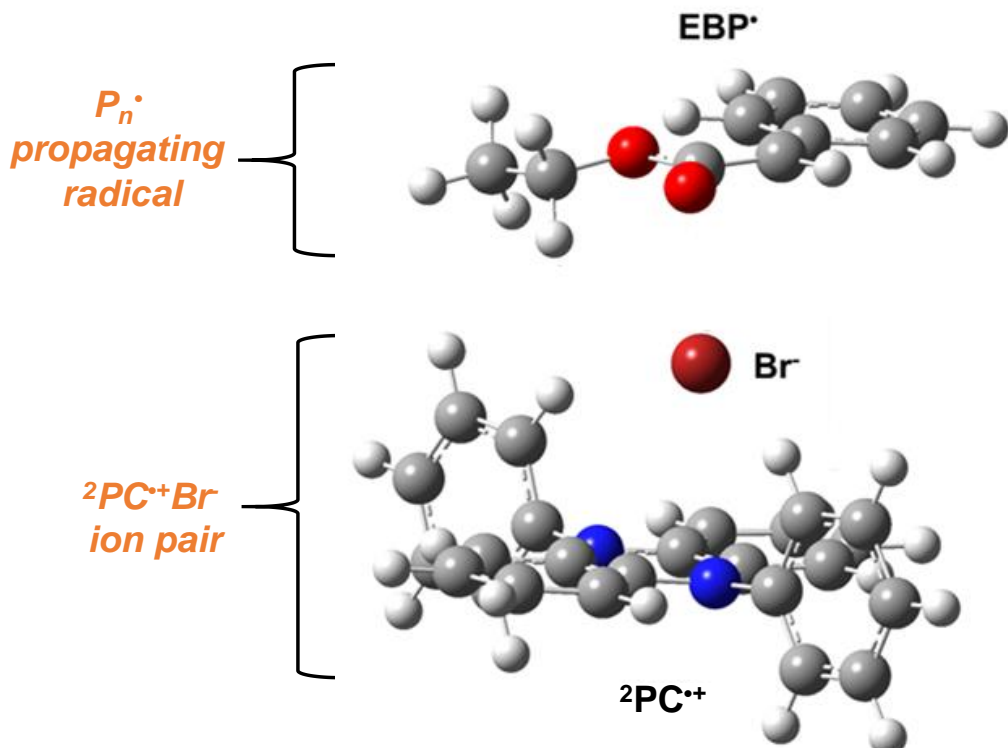


Figure S8. Proposed O-ATRP deactivation mechanism via oxidation of propagating radical ($P_n\bullet$) by ${}^2PC\bullet^+Br^-$ ion pair. $P_n\bullet$ is exemplified by neutral radical of ethyl a-bromophenylacetate (EBP) and ${}^2PC\bullet^+$ is exemplified by radical cation of 5,10-diphenyl-5,10-dihydrophenazine.

9. Oxygen Quenching on PC 3's Emission Spectrum

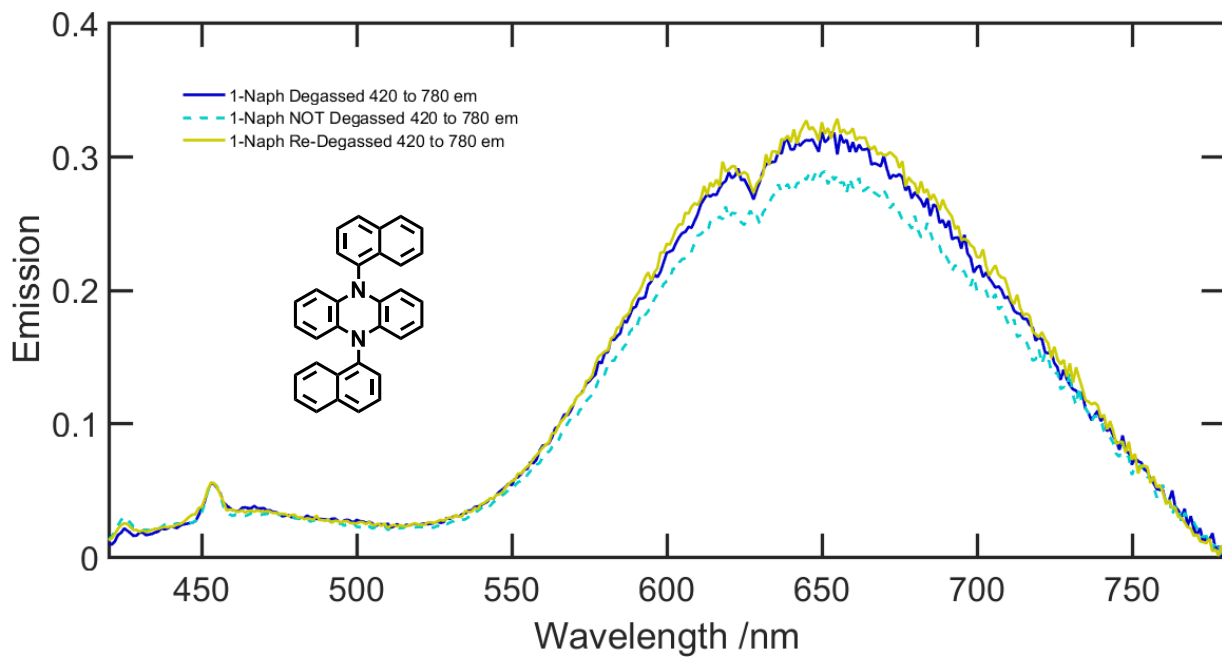


Figure S9. Introduction of oxygen minimally quenches the emission, which supports that the emission is due to fluorescence from the lowest singlet excited state.

10. Coordinates of Molecular Structures

All coordinates are reported as XYZ Cartesian coordinates. Converged geometries were obtained from uM06/6-31+G** level of theory in CPCM-described solvents (DMA or THF). Single point energies computed at uM06/6-31+G** level of theory (reported in parentheses) are arranged in the following order: E_{0K} (not ZPE and thermally corrected), H (298.15 K, 1atm), G^{0*} (298.15K, 1atm), and G⁰ (298.15K, 1M). They are stated in Hartrees units. All energies reported were calculated using the GAUSSIAN 09 ver. D.01 computational chemistry package.

a) Br⁻

DMA solvent (-2574.199117, -2574.196756, -2574.215292, -2574.212274)

Br -3.89062 2.11056 3.84586

THF solvent (-2574.187588, -2574.185227, -2574.203763, -2574.200745)

Br -3.89062 2.11056 3.84586

b) ²PC^{*}+Br⁻ (PC 3)

DMA solvent (-3915.519316, -3915.044939, -3915.135648, -3915.13263)

C	-6.67223	-0.14732	-0.21807
C	-5.31022	-0.11830	0.00578
C	-4.67740	1.08346	0.35938
C	-5.44474	2.26991	0.46538
C	-6.82566	2.22160	0.21853
C	-7.43211	1.02608	-0.11138
C	-3.45576	3.50760	1.03045
C	-2.68724	2.32132	0.92097
C	-1.31578	2.35917	1.21744
H	-0.72824	1.44895	1.15123
C	-0.71859	3.54352	1.59703
C	-1.47854	4.71862	1.70103
C	-2.83069	4.69991	1.42795
H	-7.15042	-1.08472	-0.48636
H	-4.72046	-1.02546	-0.08414
H	-7.41551	3.12975	0.29293
H	-8.50190	1.00201	-0.29604
H	0.34291	3.55860	1.82547
H	-1.00747	5.64749	2.00872
H	-3.42138	5.60588	1.52229
N	-4.81077	3.45945	0.77394
N	-3.31204	1.14165	0.56838
Br	-4.32196	1.87850	3.87399
C	-5.60946	4.64279	0.96655
C	-5.85428	5.48939	-0.14453
C	-6.12087	4.89388	2.21473
C	-5.33333	5.24196	-1.43897
C	-6.67548	6.63563	0.07385
C	-6.92689	6.03471	2.41610
H	-5.89357	4.20068	3.02568
C	-5.61931	6.09822	-2.47463
H	-4.70687	4.36796	-1.60817
C	-6.94865	7.49630	-1.01889
C	-7.19790	6.88161	1.36869
H	-7.33318	6.23395	3.40381

C	-6.43386	7.23474	-2.26466
H	-5.21616	5.90263	-3.46502
H	-7.57643	8.36920	-0.84943
H	-7.82337	7.75980	1.51816
H	-6.65087	7.90110	-3.09548
C	-2.54906	-0.08052	0.57751
C	-1.91891	-0.50574	-0.61946
C	-2.45136	-0.77878	1.75486
C	-2.00979	0.20560	-1.84171
C	-1.15822	-1.71190	-0.56493
C	-1.69876	-1.97169	1.79113
H	-2.95215	-0.38782	2.64208
C	-1.37075	-0.26356	-2.96389
H	-2.59007	1.12559	-1.88559
C	-0.51116	-2.16340	-1.74265
C	-1.06760	-2.42387	0.65766
H	-1.61945	-2.52556	2.72240
C	-0.61394	-1.45680	-2.91549
H	-1.44521	0.28723	-3.89812
H	0.07033	-3.08248	-1.69794
H	-0.48202	-3.34118	0.68175
H	-0.11327	-1.81200	-3.81251

THF solvent (-3915.513707, -3915.039018, -3915.129317, -3915.126298)

C	-6.73237	-0.36441	0.67262
C	-5.35588	-0.28956	0.74173
C	-4.72923	0.93410	1.02134
C	-5.52020	2.09289	1.22218
C	-6.91751	1.99789	1.13536
C	-7.51520	0.78235	0.87030
C	-3.52689	3.38046	1.64381
C	-2.73639	2.22114	1.44459
C	-1.34434	2.30062	1.60261
H	-0.73688	1.41367	1.45372
C	-0.75241	3.49652	1.95517
C	-1.53518	4.64317	2.15411
C	-2.90548	4.58769	1.99737
H	-7.20652	-1.31882	0.46349
H	-4.74985	-1.17736	0.59003
H	-7.52473	2.88444	1.28842
H	-8.59779	0.71965	0.81329
H	0.32535	3.54396	2.07920
H	-1.06616	5.58209	2.43316
H	-3.51164	5.47428	2.15541
N	-4.89282	3.30069	1.45725
N	-3.35360	1.04356	1.07181
Br	-4.29672	1.44687	4.37403
C	-5.69375	4.48181	1.63174
C	-5.98253	5.27325	0.49125
C	-6.15013	4.79616	2.88637
C	-5.51570	4.95974	-0.81012
C	-6.78587	6.43544	0.68745
C	-6.94099	5.95109	3.06578
H	-5.89193	4.14483	3.72143
C	-5.83786	5.76964	-1.87216
H	-4.90054	4.07439	-0.96443

C	-7.09789	7.24613	-0.43269
C	-7.25000	6.74854	1.99025
H	-7.30293	6.20191	4.05888
C	-6.63588	6.92155	-1.68413
H	-5.47691	5.52429	-2.86780
H	-7.71229	8.13150	-0.27969
H	-7.86120	7.63940	2.12305
H	-6.88189	7.54930	-2.53672
C	-2.54825	-0.12641	0.84748
C	-2.11266	-0.39928	-0.47408
C	-2.22699	-0.92658	1.91434
C	-2.43762	0.42085	-1.58368
C	-1.31061	-1.56210	-0.67146
C	-1.43064	-2.07257	1.70342
H	-2.59376	-0.65596	2.90497
C	-1.98432	0.09437	-2.83871
H	-3.04963	1.30973	-1.43671
C	-0.86128	-1.86627	-1.98102
C	-0.98550	-2.37983	0.44036
H	-1.17349	-2.70689	2.54707
C	-1.19014	-1.05781	-3.04105
H	-2.23787	0.72597	-3.68638
H	-0.24999	-2.75477	-2.12859
H	-0.37119	-3.26266	0.27289
H	-0.84079	-1.30039	-4.04136

c) $^2\text{PC}^{\bullet+}$ (PC 3)

DMA solvent (-1341.308536, -1340.835929, -1340.916642, -1340.913624)

C	-6.76872	-0.25821	0.18681
C	-5.40010	-0.22514	0.35792
C	-4.75350	0.98911	0.63736
C	-5.51841	2.17930	0.74036
C	-6.90966	2.12325	0.55908
C	-7.52529	0.91913	0.28676
C	-3.50326	3.43720	1.17888
C	-2.73825	2.24724	1.07559
C	-1.34482	2.30692	1.23967
H	-0.75687	1.39787	1.16304
C	-0.72787	3.51307	1.49970
C	-1.48460	4.69000	1.60024
C	-2.85457	4.65427	1.44170
H	-7.25781	-1.20384	-0.02683
H	-4.81398	-1.13569	0.28076
H	-7.49596	3.03355	0.63484
H	-8.60186	0.88789	0.14966
H	0.35008	3.54608	1.62497
H	-0.99482	5.63778	1.80249
H	-3.44010	5.56505	1.51882
N	-4.87566	3.37669	1.00461
N	-3.38005	1.05114	0.80112
C	-5.64325	4.59680	1.03618
C	-6.16036	5.02847	2.23070
C	-5.83108	5.30869	-0.17796
C	-6.90933	6.22368	2.27564

H	-5.98604	4.44473	3.13205
C	-6.58981	6.51581	-0.11686
C	-7.11622	6.94704	1.12678
H	-7.31768	6.56373	3.22289
C	-2.58796	-0.13667	0.60208
C	-2.12108	-0.42363	-0.70813
C	-2.29624	-0.93439	1.67868
C	-1.31942	-1.59209	-0.87488
C	-1.50255	-2.08740	1.49839
H	-2.67680	-0.66614	2.66202
C	-1.02635	-2.40399	0.24979
H	-1.27094	-2.71594	2.35331
H	-0.41110	-3.28975	0.10405
H	-7.69452	7.86864	1.15394
C	-6.79842	7.25208	-1.31015
C	-6.28249	6.81382	-2.50478
H	-6.45006	7.38503	-3.41407
C	-5.53211	5.61730	-2.55986
H	-5.12874	5.27893	-3.51077
C	-5.30856	4.87877	-1.42298
H	-4.72729	3.95932	-1.47777
H	-7.37901	8.17131	-1.26020
C	-2.41066	0.38645	-1.83422
H	-3.02342	1.27907	-1.71765
C	-0.83410	-1.90887	-2.16850
C	-1.12937	-1.10820	-3.24422
H	-0.75233	-1.36003	-4.23198
C	-1.92452	0.04791	-3.07382
H	-2.15343	0.67378	-3.93244
H	-0.22209	-2.80056	-2.29022

THF solvent (-1341.303108, -1340.830596, -1340.910828, -1340.90781)

C	-0.70150	-3.61988	-0.73835
C	-1.39945	-2.42997	-0.75063
C	-0.70918	-1.20729	-0.76396
C	0.70914	-1.20732	-0.76394
C	1.39937	-2.43001	-0.75058
C	0.70139	-3.61990	-0.73832
C	0.70918	1.20833	-0.76235
C	-0.70913	1.20835	-0.76236
C	-1.39937	2.43101	-0.74743
H	-2.48479	2.43210	-0.74713
C	-0.70138	3.62089	-0.73360
C	0.70151	3.62086	-0.73358
C	1.39945	2.43097	-0.74741
H	-1.24652	-4.55896	-0.72779
H	-2.48487	-2.43102	-0.75034
H	2.48479	-2.43110	-0.75025
H	1.24637	-4.55900	-0.72773
H	-1.24638	4.55996	-0.72179
H	1.24653	4.55992	-0.72177
H	2.48488	2.43202	-0.74709
N	1.38620	0.00050	-0.77113
N	-1.38619	0.00055	-0.77115
C	2.82766	0.00048	-0.74353
C	3.51480	0.00125	-1.93049

C	3.48281	-0.00034	0.51602
C	4.92567	0.00121	-1.92059
H	2.96391	0.00188	-2.86878
C	4.90956	-0.00037	0.51061
C	5.60306	0.00041	-0.72588
H	5.46721	0.00181	-2.86207
C	-2.82765	0.00061	-0.74353
C	-3.48281	-0.00035	0.51602
C	-3.51479	0.00160	-1.93049
C	-4.90956	-0.00031	0.51060
C	-4.92566	0.00163	-1.92060
H	-2.96389	0.00234	-2.86878
C	-5.60305	0.00069	-0.72589
H	-5.46719	0.00239	-2.86208
H	-6.69115	0.00070	-0.71044
H	6.69116	0.00037	-0.71043
C	5.59755	-0.00117	1.75003
C	4.90619	-0.00192	2.93611
H	5.44332	-0.00254	3.88090
C	3.49292	-0.00189	2.93601
H	2.95606	-0.00248	3.88111
C	2.79266	-0.00112	1.75387
H	1.70359	-0.00112	1.76778
H	6.68573	-0.00120	1.74099
C	-2.79268	-0.00139	1.75389
H	-1.70361	-0.00148	1.76783
C	-5.59756	-0.00128	1.75001
C	-4.90622	-0.00226	2.93610
H	-5.44337	-0.00300	3.88088
C	-3.49295	-0.00231	2.93602
H	-2.95610	-0.00310	3.88112
H	-6.68574	-0.00125	1.74096

d) NBu₄⁺Br⁻

DMA solvent (-3259.813448, -3259.285106, -3259.37108, -3259.368062)

C	-0.73729	-0.75440	-1.32447
H	-1.54996	-0.08898	-1.00438
C	1.52273	-1.40864	-0.59166
H	1.11143	-2.31084	-0.12634
C	0.92399	0.98608	-1.07203
H	0.00389	1.48334	-1.40190
H	1.50847	0.71714	-1.96140
C	0.04537	-0.08574	0.96584
H	-0.55241	0.83229	0.93198
H	0.96845	0.12224	1.51616
N	0.45880	-0.34268	-0.46935
Br	-2.45475	2.28525	-0.02012
H	1.61637	-1.60785	-1.66717
H	-0.46900	-0.47288	-2.35013
C	1.68275	1.95652	-0.18738
H	1.04591	2.29262	0.64158
H	2.58135	1.51261	0.25778
C	2.88660	-1.10696	-0.00801
H	3.36785	-0.28159	-0.54978

H	2.81547	-0.80821	1.04744
C	-1.16562	-2.21116	-1.32336
H	-0.46433	-2.82257	-1.90752
H	-1.20057	-2.64536	-0.31827
C	-0.74310	-1.15662	1.68611
H	-1.74088	-1.27028	1.23703
H	-0.24680	-2.13733	1.65118
C	-2.55684	-2.30992	-1.94391
H	-2.56006	-1.80472	-2.92125
H	-3.26813	-1.75588	-1.31176
C	2.07718	3.17345	-1.01879
H	1.17246	3.60784	-1.47093
H	2.71796	2.85719	-1.85502
C	2.79177	4.22180	-0.18301
H	3.06104	5.09851	-0.78135
H	2.15719	4.56299	0.64452
H	3.71456	3.81734	0.25154
C	-3.00892	-3.75135	-2.10261
H	-4.01481	-3.81386	-2.53072
H	-2.32977	-4.30708	-2.76111
H	-3.02475	-4.26605	-1.13361
C	3.76999	-2.34659	-0.11049
H	3.82471	-2.66948	-1.16041
H	3.29954	-3.17331	0.44130
C	5.16834	-2.09280	0.42699
H	5.79415	-2.98857	0.35783
H	5.66688	-1.29206	-0.13337
H	5.13535	-1.78840	1.48063
C	-0.90813	-0.73401	3.14297
H	-1.35047	0.27377	3.17395
H	0.08312	-0.64918	3.61151
C	-1.77577	-1.70245	3.92780
H	-1.88817	-1.38698	4.97032
H	-2.77883	-1.77503	3.48923
H	-1.34078	-2.70989	3.92802

THF solvent (-3259.808068, -3259.279549, -3259.364557, -3259.361538)

C	-0.75836	-0.72228	-1.32238
H	-1.54898	-0.03184	-0.99962
C	1.48181	-1.44500	-0.59478
H	1.04430	-2.33637	-0.13187
C	0.95348	0.96840	-1.06685
H	0.04675	1.49522	-1.38801
H	1.52627	0.68631	-1.96002
C	0.04832	-0.08383	0.96939
H	-0.51967	0.85313	0.93905
H	0.97871	0.09025	1.51939
N	0.45149	-0.34884	-0.46797
Br	-2.37667	2.31848	-0.03118
H	1.56889	-1.64456	-1.67100
H	-0.48252	-0.44556	-2.34748
C	1.74423	1.91132	-0.18014
H	1.12028	2.25975	0.65336
H	2.63317	1.44020	0.25763
C	2.85496	-1.18747	-0.01125
H	3.36025	-0.37454	-0.54982

H	2.79315	-0.88937	1.04499
C	-1.22978	-2.16545	-1.32330
H	-0.55129	-2.79701	-1.91365
H	-1.27066	-2.60073	-0.31885
C	-0.77897	-1.12785	1.68510
H	-1.77781	-1.20411	1.23074
H	-0.31817	-2.12606	1.65229
C	-2.62785	-2.21913	-1.93415
H	-2.62036	-1.71547	-2.91230
H	-3.31508	-1.63886	-1.29919
C	2.16500	3.12358	-1.00549
H	1.26836	3.58244	-1.44919
H	2.79396	2.79819	-1.84742
C	2.90817	4.14883	-0.16598
H	3.19336	5.02399	-0.75911
H	2.28538	4.49770	0.66710
H	3.82428	3.72107	0.26058
C	-3.13037	-3.64422	-2.08746
H	-4.13884	-3.67204	-2.51299
H	-2.47334	-4.22621	-2.74589
H	-3.16302	-4.15545	-1.11701
C	3.70334	-2.45099	-0.11789
H	3.75070	-2.77082	-1.16923
H	3.20971	-3.26724	0.42939
C	5.10735	-2.23805	0.42253
H	5.70951	-3.14937	0.34789
H	5.62744	-1.44698	-0.13190
H	5.08146	-1.93996	1.47812
C	-0.93575	-0.69937	3.14118
H	-1.33456	0.32620	3.16915
H	0.05511	-0.65761	3.61670
C	-1.84986	-1.62963	3.91940
H	-1.95001	-1.31396	4.96306
H	-2.85412	-1.65151	3.47841
H	-1.46389	-2.65696	3.91610

e) NBu₄⁺

DMA solvent (-685.6036184, -685.0778359, -685.1547159, -685.1516974)

C	-1.20240	-1.53755	0.13688
H	-1.44939	-1.85606	-0.88367
C	0.13432	0.20819	1.25862
H	-0.78240	0.79846	1.34721
C	1.20129	-1.52983	-0.20323
H	0.82563	-2.38040	-0.78363
H	1.44061	-1.89797	0.80239
C	-0.13643	0.25697	-1.25559
H	-0.12917	-0.44803	-2.09632
H	0.77947	0.85169	-1.32123
N	-0.00061	-0.60211	-0.01469
H	0.12782	-0.52877	2.07124
H	-0.82364	-2.41569	0.67259
C	2.44022	-0.98887	-0.89450
H	2.25054	-0.84981	-1.96683
H	2.75739	-0.01698	-0.49966

C	1.33723	1.11771	1.38985
H	2.26720	0.53591	1.44189
H	1.42040	1.79783	0.52992
C	-2.43493	-1.02945	0.86307
H	-2.23600	-0.93929	1.93895
H	-2.75440	-0.04052	0.51596
C	-1.33979	1.17063	-1.35157
H	-2.27165	0.59308	-1.41585
H	-1.41646	1.82473	-0.47099
C	-3.57714	-2.01934	0.65106
H	-3.24796	-3.02725	0.94359
H	-3.81315	-2.07206	-0.42202
C	3.57851	-1.99014	-0.71740
H	3.24781	-2.98344	-1.05500
H	3.80636	-2.08968	0.35414
C	4.82530	-1.57247	-1.47813
H	5.63710	-2.29432	-1.34182
H	4.62339	-1.49465	-2.55353
H	5.18628	-0.59443	-1.13606
C	-4.81679	-1.62942	1.43796
H	-5.63301	-2.34116	1.27724
H	-4.60665	-1.59826	2.51415
H	-5.17528	-0.63606	1.14047
C	1.20695	1.94834	2.66350
H	1.09017	1.27606	3.52592
H	0.28680	2.54837	2.61359
C	2.40776	2.85545	2.87261
H	2.30863	3.44572	3.78932
H	3.33381	2.27217	2.94875
H	2.52368	3.55461	2.03514
C	-1.21551	2.03896	-2.60048
H	-1.11606	1.39263	-3.48457
H	-0.28865	2.62788	-2.54316
C	-2.40888	2.96466	-2.76687
H	-2.31448	3.58219	-3.66595
H	-3.34210	2.39379	-2.84961
H	-2.50671	3.63829	-1.90653

THF solvent (-685.596295, -685.0704783, -685.1473603, -685.1443418)

C	-1.20281	-1.53735	0.13718
H	-1.45003	-1.85588	-0.88345
C	0.13463	0.20837	1.25882
H	-0.78272	0.79763	1.34813
C	1.20149	-1.52978	-0.20343
H	0.82553	-2.38075	-0.78329
H	1.44120	-1.89782	0.80228
C	-0.13661	0.25737	-1.25540
H	-0.13029	-0.44768	-2.09625
H	0.78006	0.85089	-1.32174
N	-0.00064	-0.60212	-0.01457
H	0.12894	-0.52874	2.07150
H	-0.82391	-2.41583	0.67249
C	2.44071	-0.98987	-0.89504
H	2.25119	-0.85115	-1.96750
H	2.75814	-0.01779	-0.50078
C	1.33663	1.11915	1.38988

H	2.26758	0.53869	1.44023
H	1.41824	1.79998	0.53026
C	-2.43579	-1.03018	0.86333
H	-2.23713	-0.93986	1.93931
H	-2.75571	-0.04131	0.51631
C	-1.33889	1.17245	-1.35120
H	-2.27171	0.59617	-1.41369
H	-1.41396	1.82737	-0.47098
C	-3.57763	-2.02078	0.65133
H	-3.24803	-3.02867	0.94360
H	-3.81374	-2.07368	-0.42178
C	3.57896	-1.99141	-0.71767
H	3.24815	-2.98497	-1.05452
H	3.80714	-2.09056	0.35388
C	4.82567	-1.57452	-1.47891
H	5.63702	-2.29654	-1.34220
H	4.62412	-1.49764	-2.55436
H	5.18754	-0.59663	-1.13761
C	-4.81746	-1.63177	1.43830
H	-5.63294	-2.34403	1.27733
H	-4.60791	-1.60099	2.51453
H	-5.17719	-0.63885	1.14107
C	1.20690	1.94881	2.66441
H	1.09231	1.27585	3.52663
H	0.28572	2.54748	2.61644
C	2.40652	2.85764	2.87256
H	2.30752	3.44683	3.78978
H	3.33375	2.27619	2.94751
H	2.52034	3.55808	2.03597
C	-1.21508	2.03971	-2.60108
H	-1.11730	1.39263	-3.48486
H	-0.28743	2.62763	-2.54555
C	-2.40750	2.96664	-2.76701
H	-2.31308	3.58309	-3.66661
H	-3.34161	2.39723	-2.84884
H	-2.50387	3.64158	-1.90761

11. References

-
- ¹ Gaussian 09, R. D., Frisch, M. J.; Trucks, G. W.; Schlegel, H. B.; Scuseria, G. E.; Robb, M. A.; Cheeseman, J. R.; Scalmani, G.; Barone, V.; Mennucci, B.; Petersson, G. A.; Nakatsuji, H.; Caricato, M.; Li, X.; Hratchian, H. P.; Izmaylov, A. F.; Bloino, J.; Zheng, G.; Sonnenberg, J. L.; Hada, M.; Ehara, M.; Toyota, K.; Fukuda, R.; Hasegawa, J.; Ishida, M.; Nakajima, T.; Honda, Y.; Kitao, O.; Nakai, H.; Vreven, T.; Montgomery, J. A., Jr.; Peralta, J. E.; Ogliaro, F.; Bearpark, M.; Heyd, J. J.; Brothers, E.; Kudin, K. N.; Staroverov, V. N.; Kobayashi, R.; Normand, J.; Raghavachari, K.; Rendell, A.; Burant, J. C.; Iyengar, S. S.; Tomasi, J.; Cossi, M.; Rega, N.; Millam, J. M.; Klene, M.; Knox, J. E.; Cross, J. B.; Bakken, V.; Adamo, C.; Jaramillo, J.; Gomperts, R.; Stratmann, R. E.; Yazyev, O.; Austin, A. J.; Cammi, R.; Pomelli, C.; Ochterski, J. W.; Martin, R. L.; Morokuma, K.; Zakrzewski, V. G.; Voth, G. A.; Salvador, P.; Dannenberg, J. J.; Dapprich, S.; Daniels, A. D.; Farkas, Ö.; Foresman, J. B.; Ortiz, J. V.; Cioslowski, J.; Fox, D. J. Gaussian, Inc., Wallingford CT, 2009.
- ² Theriot, J. C.; Lim, C.-H.; Yang, H.; Ryan, M. D.; Musgrave, C. B.; Miyake, G. M. *Science* **2016**, 352, 1082-1086.
- ³ Zhao, Y.; Truhlar, D. *Theor. Chem. Acc.* **2008**, 120, 215-241
- ⁴ Yanai, T.; Tew, D. P.; Handy, N. C. *Chemical Physics Letters* **2004**, 393, 51-57
- ⁵ Spackman, M. A. *J. Comput. Chem.* **1996**, 17, 1-18
- ⁶ Marcus, Y.; Hefter, G. *Chem. Rev.* **2006**, 106, 4585-4621
- ⁷ Verhoeven, J. W. Sigma-coupled Charge-Transfer Probes of the Fluoroprobe and Fluorotrope Type. In Advanced Concepts in Fluorescence Sensing Part A: Small Molecule Sensing; Springer US, 2005.